

8-27-2012

High superconducting anisotropy and weak vortex pinning in Co-doped LaFeAsO

G. Li

Florida State University

G. Grissonnanche

Florida State University

J.-Q. Yan

Iowa State University

R. William McCallum

Iowa State University, mccallum@ameslab.gov

Thomas A. Lograsso

Iowa State University, lograsso@ameslab.gov

Follow this and additional works at: http://lib.dr.iastate.edu/ameslab_pubs



Part of the [Condensed Matter Physics Commons](#), and the [Materials Science and Engineering Commons](#)

The complete bibliographic information for this item can be found at http://lib.dr.iastate.edu/ameslab_pubs/37. For information on how to cite this item, please visit <http://lib.dr.iastate.edu/howtocite.html>.

High superconducting anisotropy and weak vortex pinning in Co-doped LaFeAsO

Abstract

Here, we present an electrical transport study in single crystals of $\text{LaFe}_{0.92}\text{Co}_{0.08}\text{AsO}$ ($T_c \approx 9.1$ K) under high magnetic fields. In contrast to most of the previously reported Fe based superconductors, and despite its relatively low T_c , $\text{LaFe}_{0.92}\text{Co}_{0.08}\text{AsO}$ shows a superconducting anisotropy which is comparable to those seen, for instance, in the cuprates or $\gamma_H = H_{c2ab}/H_{c2c} = m_c/m_{ab} \approx 9$, where m_c/m_{ab} is the effective-mass anisotropy, although, in the present case and as in all Fe based superconductors, $\gamma \rightarrow 1$ as $T \rightarrow 0$. Under the application of an external field, we also observe a remarkable broadening of the superconducting transition particularly for fields applied along the interplanar direction. Both observations indicate that the low dimensionality of $\text{LaFe}_{1-x}\text{Co}_x\text{AsO}$ is likely to lead to a more complex vortex phase diagram when compared to the other Fe arsenides and consequently, to a pronounced dissipation associated with the movement of vortices in a possible vortex liquid phase. When compared to, for instance, F-doped compounds pertaining to the same family, we obtain rather small activation energies for the motion of vortices. This suggests that the disorder introduced by doping LaFeAsO with F is more effective in pinning the vortices than alloying it with Co.

Disciplines

Condensed Matter Physics | Materials Science and Engineering

Comments

This article is from *Physical Review B* 86 (2012): 054517, doi:[10.1103/PhysRevB.86.054517](https://doi.org/10.1103/PhysRevB.86.054517).

Authors

G. Li, G. Grissonnanche, J.-Q. Yan, R. William McCallum, Thomas A. Lograsso, H. D. Zhou, and L. Balicas

High superconducting anisotropy and weak vortex pinning in Co-doped LaFeAsOG. Li,¹ G. Grissonnanche,¹ J.-Q. Yan,^{2,*} R. W. McCallum,² T. A. Lograsso,² H. D. Zhou,¹ and L. Balicas^{1,†}¹*National High Magnetic Field Laboratory, Florida State University, Tallahassee, Florida 32310, USA*²*Division of Materials Science and Engineering, Ames Laboratory, US-DOE, Iowa State University, Ames, Iowa 50011, USA*

(Received 22 June 2012; published 27 August 2012)

Here, we present an electrical transport study in single crystals of LaFe_{0.92}Co_{0.08}AsO ($T_c \simeq 9.1$ K) under high magnetic fields. In contrast to most of the previously reported Fe based superconductors, and despite its relatively low T_c , LaFe_{0.92}Co_{0.08}AsO shows a superconducting anisotropy which is comparable to those seen, for instance, in the cuprates or $\gamma_H = H_{c2}^{ab}/H_{c2}^c = m_c/m_{ab} \simeq 9$, where m_c/m_{ab} is the effective-mass anisotropy, although, in the present case and as in all Fe based superconductors, $\gamma \rightarrow 1$ as $T \rightarrow 0$. Under the application of an external field, we also observe a remarkable broadening of the superconducting transition particularly for fields applied along the interplanar direction. Both observations indicate that the low dimensionality of LaFe_{1-x}Co_xAsO is likely to lead to a more complex vortex phase diagram when compared to the other Fe arsenides and consequently, to a pronounced dissipation associated with the movement of vortices in a possible vortex liquid phase. When compared to, for instance, F-doped compounds pertaining to the same family, we obtain rather small activation energies for the motion of vortices. This suggests that the disorder introduced by doping LaFeAsO with F is more effective in pinning the vortices than alloying it with Co.

DOI: [10.1103/PhysRevB.86.054517](https://doi.org/10.1103/PhysRevB.86.054517)

PACS number(s): 74.70.Xa, 74.25.Dw, 74.62.Dh, 74.25.fc

I. INTRODUCTION

LaFePO was the first Fe-based pnictide compound to display a superconducting ground state at a transition temperature $T_c \simeq 7$ K.¹ Soon after this discovery, Kamihara *et al.*² found the emergence of superconductivity, with a maximum T_c of 26 K, by doping its isostructural compound LaFeAsO with F. The first reported phase diagram² comprises an antiferromagnetic metallic ground state that is progressively suppressed by F doping, which is found to produce a superconducting dome as previously observed in the cuprates (as a function of hole doping). The boundary between antiferromagnetic and superconducting states suggests the coexistence between both phases although a subsequent phase diagram as a function of F content derived from either muon scattering³ or thermal-expansion measurements⁴ in polycrystalline material, indicates what seemingly is a first-order phase boundary between antiferromagnetic and superconducting phases with virtually no overlap between both states.

Soon after its discovery, the superconducting state in LaFeAsO_{1-x}F_x was recognized to be unconventional. The experimental evidence includes (i) the absence of a coherence peak and the observation of a power law in the nuclear magnetic resonance (NMR) relaxation rate within the superconducting state,⁵ (ii) the ratio of the superconducting transition temperature T_c to the superfluid density is close to the so-called Uemura line for the high- T_c cuprates,⁶ (iii) an unconventional phase boundary between superconducting and metallic states under high magnetic fields claimed to result from a multigap superconducting state,⁷ (iv) the presence of pronounced antiferromagnetic spin fluctuations at temperatures above the superconducting transition temperature (T_c) whose strength “tracks” T_c ,⁸ and (v) the existence of a pseudogaplike phase preceding superconductivity.^{9–12} Electronic anisotropy,¹³ proximity to antiferromagnetism, pronounced antiferromagnetic spin fluctuations within the superconducting and metallic phases, and the existence of a pseudogap state

whose relation with the superconductivity is poorly understood are all known properties of the high- T_c cuprates.¹⁴

Nevertheless, a characteristic feature of the cuprates is the broadening of the resistive transition in the presence of a magnetic field. Initial investigations of the resistive transition in their so-called mixed state¹⁵ indicated a current-independent, thermally activated behavior, i.e., $\rho \sim \rho_0 \exp(-U_0/T)$, with U_0 ranging from 10⁴ K at high magnetic fields (for $H \simeq 10$ K) to 10⁵ K (for $H \ll 10$ K). Transport studies^{16,17} also revealed a characteristic temperature T_g above which the current-voltage (IV) characteristics is linear, but becomes extremely nonlinear below T_g : $V \propto \exp(-A/I^\alpha)$. This observation was attributed to a transition between an unpinned viscous regime, or vortex-liquid to a pinned regime, i.e., a vortex glass state, characterized by a limited motion of vortex lines. T_g has been found to coincide with the irreversibility line as extracted from magnetometry measurements.¹⁷ In the vortex liquid regime and at lower temperatures the resistivity ρ was found to display an activated behavior: $\rho \propto \exp(-U_0/T)$ with $U_0(T_k) \gg T_k$.

Here, we report electrical transport measurements in Co-doped LaFeAsO samples in order to extract the phase boundary between superconducting and metallic states as a function of magnetic field (H) and temperature (T). The resulting phase diagram reveals a marked superconducting anisotropy $\gamma^{1/2} = H_{c2}^{ab}/H_{c2}^c = (m_c/m_{ab})^{1/2} \simeq 9$ in the neighborhood of T_c . This value for γ is considerably larger than the values reported for other Fe based superconductors such as Ba_{1-x}K_xFe₂As₂,¹⁸ NdFeAsO_{0.7}F_{0.3},¹⁹ K_{0.8}Fe_{1.76}Se₂,²⁰ and even Ca₁₀(Pt₄As₈)(Fe_{1-x}Pt_x)₂As₂.²¹ Although, as found in most Fe pnictides, γ progressively tends to a value close to 1 as $T \rightarrow 0$ K, suggesting that the Pauli limiting mechanism, in contrast to the orbital effect, becomes the dominant pair breaking mechanism at low temperatures. Similarly to what is known from the family of cuprate superconductors, one observes a pronounced field-induced increase in the width of the resistive transition as a function of T particularly for fields applied along the c -axis. An Arrhenius plot of the resistance as

a function of temperature leads to extremely small values for the activation energy U_0 for vortex motion, i.e., between 10^1 and 10^2 K. Values in the order of 10^2 K are obtained for fields applied along the ab plane. These values contrast markedly with those measured in $\text{NdFeAsO}_{0.7}\text{F}_{0.3}$,¹⁹ and with the large critical currents obtained in $\text{SmFeAsO}_{1-x}\text{F}_x$ single-crystals,²² indicating that Co is far less effective than F in pinning vortices.

II. EXPERIMENT

LaFeAsO single crystals were synthesized in a NaAs flux at ambient pressure as described in Ref. 23. The quality of the so-obtained crystals was previously characterized by Laue backscattering, x-ray powder diffraction, magnetization, and resistivity measurements. The Co content was determined by using wavelength dispersive x-ray spectroscopy (WDS) in a JEOL JXA-8200 Superprobe electron probe microanalyzer (EPMA). Resistivity measurements under field were performed by using a conventional four-terminal ac technique in either a physical parameter measurement system or a Bitter resistive magnet, coupled to variable temperature insert, which is capable of reaching a field of 35 T.

Figure 1 shows the resistivity ρ for $\text{LaFe}_{0.92}\text{Co}_{0.08}\text{AsO}$ single crystal, for current flowing within the planes as a function of temperature and in absence of an externally applied field. One observes no clear indications for a phase transition, such as the orthorhombic distortion, or the antiferromagnetism seen in the parent compound.¹⁻³ The resistivity ratio in the metallic state $\rho(300\text{ K})/\rho(10\text{ K}) < 2$ is rather small suggesting that alloying with Co produces a considerable amount of disorder and it is an effective source of quasiparticle scattering. For this level of Co doping the onset of the resistive transition is seen at $T_c \simeq 9.4\text{ K}$, with a transition width $\Delta T_c = T_c(90\% \rho_n) - T_c(10\% \rho_n) \simeq 1\text{ K}$, where ρ_n is the resistivity in the metallic state just above the transition.

Figure 2 shows the resistive transition for a $\text{LaFe}_{0.92}\text{Co}_{0.08}\text{AsO}$ single crystal as a function of the temperature for several values of the magnetic field up to 9 T, applied either along the ab plane (top panel) or along the c axis (bottom panel). While 9 T only suppresses T_c by

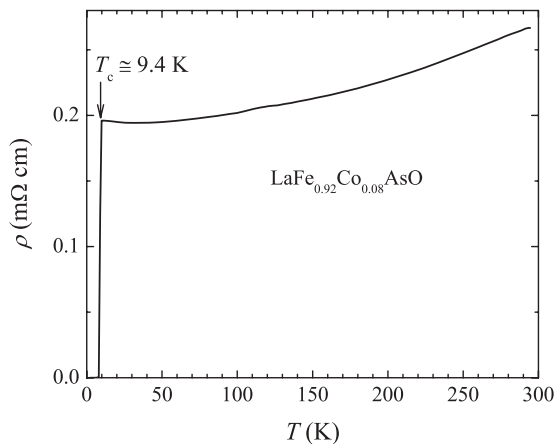


FIG. 1. Resistivity ρ as a function of temperature T for a Co-doped LaFeAsO single crystal. The superconducting transition temperature T_c is indicated by the vertical arrow. No evidence for either a structural or a magnetic phase transition is observed.

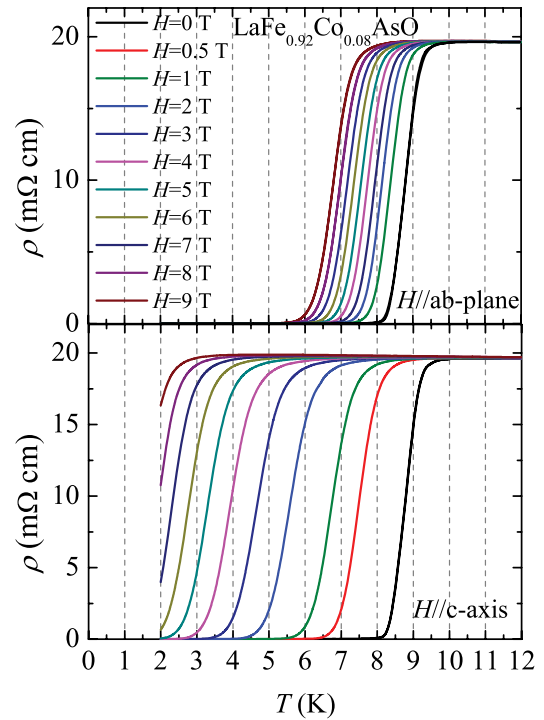


FIG. 2. (Color online) Top panel: Resistivity ρ as a function of temperature T for a $\text{LaFe}_{0.92}\text{Co}_{0.08}\text{AsO}$ single crystal measured under several values of the magnetic field H applied along a planar direction. Bottom panel: Same as in the top panel but for fields applied along the c axis.

approximately 2 K for fields along the ab plane, for fields along the c axis the superconducting transition is seen to shift considerably to lower temperatures, and under a field of 9 T, the transition temperature has shifted to temperatures below 2 K. For fields along either direction, one observes what seemingly are parallel resistive transition curves, as usually seen in conventional superconductors, whose displacement in temperature is strongly orientation dependent.

In order to construct the superconducting phase diagram of $\text{LaFe}_{0.92}\text{Co}_{0.08}\text{AsO}$, as seen in Fig. 3, we measured the resistive transition at several temperatures and as a function of the applied field oriented either along the ab plane (top panel) or along the c axis (lower panel). As seen in Fig. 3, for fields aligned along the ab plane, the resistive transition is just displaced to higher fields as T is lowered, producing a set of nearly parallel resistive transition curves. But for fields oriented along the c axis (lower panel of Fig. 3) the width of the resistive transition is seen to increase as the T is lowered. At first glance this would seem to be surprising since fluctuations should become less prominent as the temperature is lowered, and therefore one would naively expect the transition to sharpen as it is effectively seen, for instance, in $\text{FeTe}_{1-x}\text{Se}_x$.²⁴ However, such a broadening is commonly observed in the regime of thermally activated flux flow of vortices²⁵ which leads to a linearly dependent flux-flow resistivity behaving as $\rho_{\text{flow}} \simeq \rho_n B/H_{c2}$, i.e., the larger the upper critical field, or the lower the temperature, the smaller is the slope B/H_{c2} as seen by us. ρ_n is again the resistivity in the metallic state preceding the transition which, as previously stated, displays a weak

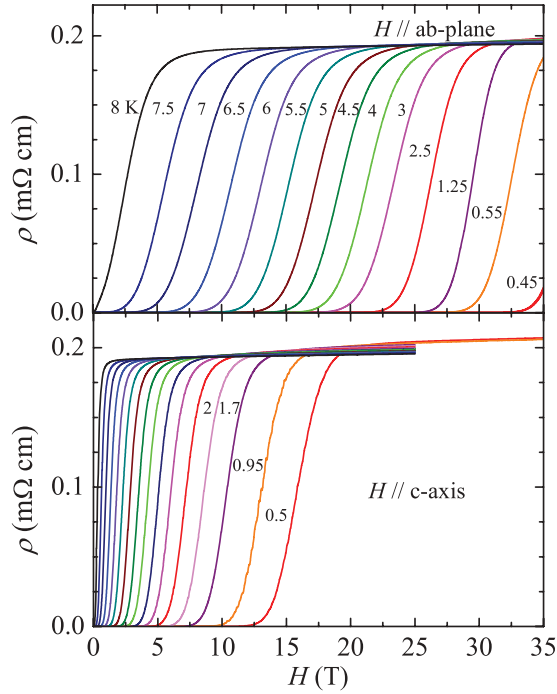


FIG. 3. (Color online) Top panel: ρ as a function of the magnetic field for a $\text{LaFe}_{0.92}\text{Co}_{0.8}\text{AsO}$ single crystal and for several values of the temperature T . Bottom panel: Same as in the top panel but for fields applied along the c axis.

field and temperature dependence. This would indicate that the energy barriers U_0 for the flow of vortices are effectively lower than the temperature at which the resistivity is measured.²⁶

The resulting superconducting phase diagram is shown in Fig. 4, where we used the middle point of the resistive transition, i.e., $T_c^m = T(0.5\rho_n)$, with ρ_n being the resistivity in the metallic state preceding the temperature-dependent resistive transition, or the value where ρ_n starts to deviate from the behavior displayed by the metallic state magnetoresistivity $[\rho_n(H)]$. $\rho_n(H)$ was adjusted to a second-degree polynomial. As seen in Fig. 4 the upper critical field for fields applied along the ab plane H_{c2}^{ab} follows a concave down curvature which extrapolates to $H_{c2}^{ab}(T = 0 \text{ K}) = \phi_0/(2\pi\xi_{ab}\xi_c) \sim 32.5 \text{ K}$, which corresponds to $\xi_{ab}\xi_c \sim 1014 \text{ \AA}^2$ where ξ_{ab} is the in-plane superconducting coherence length and ξ_c is the interplane one. As for fields applied along the c axis, one observes the usual concave-up curvature for $H_{c2}^c(T)$ claimed to result from multiband superconductivity,⁷ and whose extrapolation to zero temperature seems to saturate at a value of $\sim 20 \text{ T}$ corresponding to $\xi_{ab} \sim 40.6 \text{ \AA}$ and therefore implying $\xi_c \sim 25 \text{ \AA}$ which is considerably larger than the inter-plane distance $c = 8.746 \text{ \AA}$.²³ The red line is a fit of $H_{c2}^{ab}(T)$ to the conventional empirical expression:

$$H_{c2}^{ab}(T) = H_{c2}^{ab}(0)[1 - (T/T_c)^2]. \quad (1)$$

The fit is relatively poor at low temperatures and yields a lower value for $H_{c2}^{ab}(0) \simeq 29.9 \text{ T}$, corresponding to $\xi_{ab}\xi_c \sim 1102 \text{ \AA}^2$. The deviation with respect to conventional behavior is rather intriguing and bears resemblance with a previous report in $\text{Fe}_{1+y}\text{Te}_{1-x}\text{Se}_x$,²⁴ where an upturn is observed in

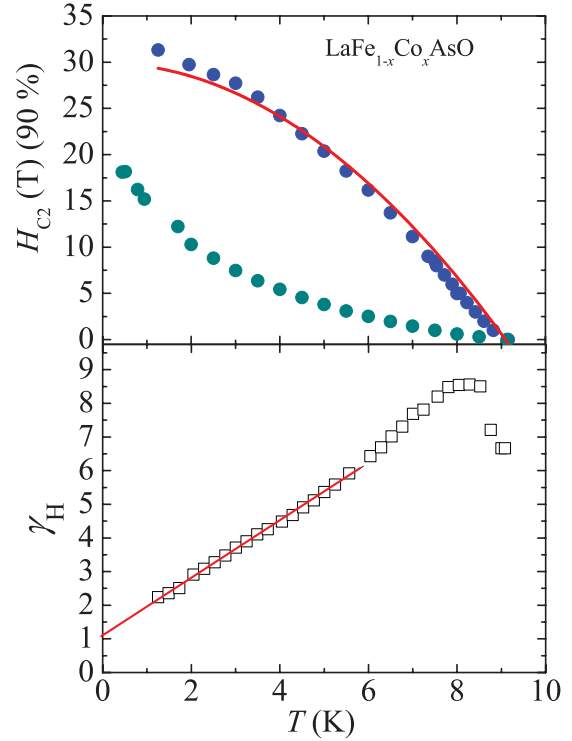


FIG. 4. (Color online) Top panel: Magnetic field as a function of the temperature superconducting to metallic phase boundary for a $\text{LaFe}_{1-x}\text{Co}_x\text{AsO}$ single crystal, and respectively for fields applied along the interplanar direction (magenta markers) and along a planar direction (blue markers). To determine the phase boundary, we used the 50% of the value of the resistance in the normal state as the criteria (see text). Lower panel: Superconducting anisotropy $\gamma_H = H_{c2}^{ab}/H_{c2}^c$ as a function of temperature. Red line is a linear fit which extrapolates to $\gamma_H \simeq 1$ as $T \rightarrow 0$.

$H_{c2}(T)$ at low temperatures and which was interpreted as evidence for an additional phase transition, the so-called Fulde-Ferrell-Larkin-Ovchinnikov (FFLO) superconducting state.²⁷ This deviation represents extremely weak evidence for an additional superconducting state, although the upper critical field in this material is considerably larger than the weak-coupling Pauli limiting field value $H_p = \Delta_0/2\mu_B$ with $\Delta_0 = 1.75k_B T_c$ which leads to the standard expression $H_p/T_c = 1.84 \text{ T/K}$, i.e., $T_c \simeq 9.4 \text{ K}$ leads to $H_p \simeq 17.3 \text{ T}$. This value is nearly a factor of 2 smaller than the extrapolation to zero temperature of the experimentally observed upper-critical field for fields along the ab plane. This could be understood if the correlations were particularly strong in this system renormalizing H_{c2} considerably, and therefore implying that this system might indeed be Pauli limited. Under such circumstances additional superconducting phases such as the FFLO state become a possibility.

The lower panel of Fig. 4 shows the resulting temperature dependence for the anisotropy in upper critical field $\gamma_H = H_{c2}^{ab}/H_{c2}^c$ which reflects the anisotropy in the effective band mass. It is observed to initially increase up to a value of $\simeq 9$ close to T_c , which is nearly twice the value of 4–5 previously reported for a “1111” compound,¹⁹ but γ quickly decreases with further decreasing the temperature and a simple

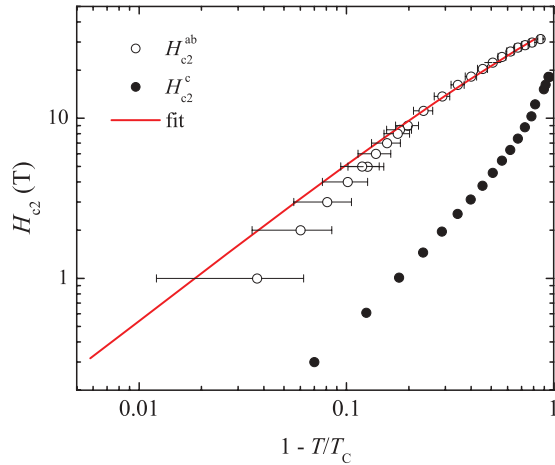


FIG. 5. (Color online) Upper critical fields H_{c2}^c (solid markers) and H_{c2}^{ab} (open markers) as a function of $1 - t$ where $t = T/T_c$. Red line is a fit of H_{c2}^c to Eq. (1) which yields a Pauli limiting field $H_p^{\parallel ab} = (64 \pm 11)$ T, and an orbital limiting field $H_0^{\parallel ab} = (54.6 \pm 3.1)$ T corresponding to $\xi_c \xi_{ab} = (603 \pm 34) \text{ \AA}^2$.

linear extrapolation suggests an isotropic system in the limit of zero temperature. This temperature-dependent behavior, which is seen in virtually all Fe based superconductors, can be understood if one assumes that the orbital limiting field is the dominant pair-breaking effect at higher temperatures. But the Pauli limiting field, which depends on the value of the superconducting gap and on the anisotropy of the Landé g factor, becomes the dominant one at low temperatures (relative to T_c) if the g factor was nearly isotropic. This would further indicate that this system is Pauli limited. To date, and to our knowledge, this is the superconducting phase diagram extracted over the widest range in reduced temperature $t = T/T_c$ for a 1111 Fe arsenide compound.

In order to evaluate the contributions of both orbital and Pauli pair-breaking effects, and in order to evaluate the so-called Maki parameter $\alpha_M = \sqrt{2}H_0/H_p$, where H_0 is the orbital limiting field, we analyze our $H_{c2}(T)$ data at temperatures close to T_c where the Ginzburg-Landau (GL) theory yields Ref. 28:

$$\left(\frac{H}{H_p}\right)^2 + \frac{H}{H_0} = 1 - \frac{T}{T_c}. \quad (2)$$

Very close to the critical temperature, $(T_c - T)/T_c \ll (H_p/H_0)^2$, the first paramagnetic term in the left-hand side is negligible and Eq. (2) yields the orbital linear GL temperature dependence, $H_{c2} = H_0(1 - T/T_c)$. At lower temperatures, $(T_c - T)/T_c > (H_p/H_0)^2$, the Pauli limiting field H_p dominates the shape of $H_{c2}(T) \propto (1 - t)^{1/2}$ even in the GL domain if $H_p < H_0$. The latter inequality is equivalent to the condition that the Maki parameter $\alpha_M \sim H_0/H_p > 1$ is large enough, assuring that the paramagnetic effects are essential. Shown in Fig. 5 are the log-log plot of our $H_{c2}(T)$ as a function of $1 - T/T_c$ where the red line is a fit to Eq. (2). Given the unconventional concave up curvature for fields applied along the c axis, this fit can only be applied to the data where the field is oriented along the ab plane. The fit is excellent for the high-field region, but less so for temperatures

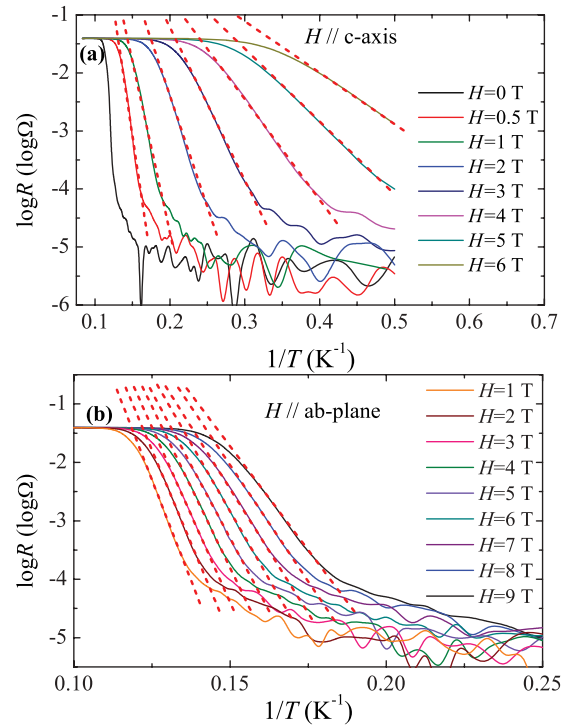


FIG. 6. (Color online) (a) Logarithm of the resistance as a function of the inverse of the temperature T^{-1} for fields applied along the c axis. (b) Same as in (a) but for fields along the ab plane. Dotted red lines are guides to the eyes, indicating a region in T^{-1} where the resistance across the superconducting transition clearly displays activated behavior.

close to T_c , probably due to the relatively large error bars in determining the temperature ($\Delta T \sim 25$ mK) which are inherent to transport measurements. It might also be attributed to the broadening of the resistive transition due to local T_c inhomogeneities. The fit yields $H_p^{\parallel ab} = (64 \pm 11)$ T for the Pauli limiting field, and $H_0^{\parallel ab} = (54.63 \pm 3.1)$ T for the orbital limiting field. Therefore the fit yields values that are comparable in magnitude, making it difficult to distinguish or evaluate the dominant pair breaking mechanism at low temperatures, and hence suggesting a Maki parameter close to unity, which is nearly beyond the validity of Eq. (2). Defining the effective Ginzburg-Landau coherence lengths, $\xi_{ab}(T) = \xi_{ab}(1 - T/T_c)^{-1/2}$ and $\xi_c(T) = \xi_c(1 - T/T_c)^{-1/2}$, we obtain $\xi_c \xi_{ab} = (\phi_0/2\pi H_0^{\parallel ab}) = (603 \pm 34) \text{ \AA}^2$, which is considerably smaller than the value of 1014 \AA^2 estimated from H_{c2}^{ab} .

Given the relatively large superconducting anisotropy observed here, comparable, for instance, to values reported for the least anisotropic cuprates, it is pertinent to ask if it would have any significant effect on the vortex phase diagram of this material. In effect, Figs. 6(a) and 6(b) show the logarithm of the resistance ($\log R$), as it decreases through the superconducting transition, and as a function of the inverse of the temperature T^{-1} for several values of the magnetic field applied either along the c axis or along an in-plane direction, respectively. As seen for over two decades in temperature $\log R$ is linear in T^{-1} allowing us to extract the field dependence of the activation

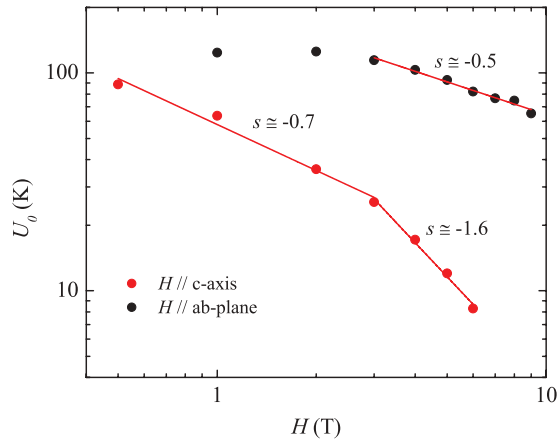


FIG. 7. (Color online) Activation energies as a function of the magnetic field as extracted from the Arrhenius plots in Figs. 6(a) and 6(b), respectively, for $H \parallel c$ axis (red markers) and for $H \parallel ab$ plane (black markers). Red lines are linear fits indicating the respective power laws.

energy U_0 . The zero-field curve does not display any clear linear dependence over a significant range in temperatures. The saturation observed at lower temperatures is mostly due to the noise floor of our instrumental setup, and probably also to a crossover towards a pinned vortex regime, i.e., the vortex-solid state.

Figure 7 shows the resulting field dependence for the activation energy U_0 for both orientations of the external field. What is remarkable in the present case is the extremely small values of U_0 which are nearly 2 to 3 orders of magnitude smaller than the values reported for either the cuprates¹⁵ or the 1111 Fe pnictides.¹⁹ This result is particularly surprising, since Co is incorporated within the superconducting Fe arsenide planes, and therefore one would naively expect it to act as a quite effective point pinning center for vortices. This result is particularly difficult to understand if one considers that F^- is incorporated within the nearly electronically inert rare-earth oxide layer having an ionic radius in the order of ~ 1 Å, thus being just about 15% larger than the ionic radius of Co^{+2} which in addition is expected to be nearly magnetic. Another surprising result is the large anisotropy (nearly one order of magnitude) between the values of U_0 for fields applied

either perpendicularly or along the conducting planes. This suggests that the layered structure of this material is more effective in pinning vortices than the incorporation of about 8% of point disorder. At the moment, these observations suggest rather unconventional vortex pinning mechanisms for the Fe arsenide superconductors. This figure also shows the power-law dependence in field or $U_0 \propto H^s$, where for fields along the ab plane U_0 remains nearly constant followed by a rather weak power law with $s = -0.5$. For fields along the c axis, on the other hand, one observes a weak power law, i.e., $s = -0.7$ which crosses over to a value $s = -1.6$ when $H > 3$ T, suggesting collective creep at high fields.²⁹

III. SUMMARY

In summary, this single-crystal electrical transport study on a La based “1111” Fe-arsenide compound reveals a relatively large superconducting anisotropy, i.e., nearly two times larger than the anisotropy previously reported in a Nd-based 1111 compound,¹⁹ suggesting perhaps that a larger electronic anisotropy is in effect detrimental to the superconducting transition temperature in these compounds. Not surprisingly, anisotropies on the order 9, combined with relatively weak vortex pinning by point defects, lead to behavior akin to what is seen in the vortex-liquid phase of the cuprates.²⁶ However, the extremely small activation energies for vortex flow, as extracted here, indicate that the introduction of point defects in the FeAs planes is ineffective in pinning vortices. This is extremely difficult to understand when compared to the strong pinning reported for F-doped samples^{19,22} or for the Co-doped 122 compounds³⁰ and will require major experimental and theoretical efforts to elucidate such a contrast.

ACKNOWLEDGMENTS

The NHMFL is supported by NSF through NSF-DMR-0084173 and the State of Florida. L.B. was supported by DOE-BES through Award No. DE-SC0002613. Work done at the Ames Laboratory was supported by the US Department of Energy, Office of Basic Energy Sciences, Division of Materials Sciences and Engineering. Ames Laboratory is operated for the US Department of Energy by Iowa State University under Contract No. DE-AC02-07CH11358.

*Present address: Materials Science and Technology Division, Oak Ridge National Laboratory, Oak Ridge, Tennessee 37831, and Department of Materials Science and Engineering, University of Tennessee, Knoxville, Tennessee 37996, USA.

†balicas@magnet.fsu.edu

¹Y. Kamihara, H. Hiramatsu, M. Hirano, R. Kawamura, H. Yanagi, T. Kamiya, and H. Hosono, *J. Am. Chem. Soc.* **128**, 10012 (2006).

²Y. Kamihara, T. Watanabe, M. Hirano, and H. Hosono, *J. Am. Chem. Soc.* **130**, 3296 (2008).

³H. Luetkens, H. H. Klauss, M. Kraken, F. J. Litterst, T. Dellmann, R. Klingeler, C. Hess, R. Khasanov, A. Amato, C. Baines,

M. Kosmala, O. J. Schumann, M. Braden, J. Hamann-Borrero, N. Leps, A. Kondrat, G. Behr, J. Werner, and B. Büchner, *Nat. Mater.* **8**, 305 (2009).

⁴L. Wang, U. Köhler, N. Leps, A. Kondrat, M. Nale, A. Gasparini, A. de Visser, G. Behr, C. Hess, R. Klingeler, and B. Büchner, *Phys. Rev. B* **80**, 094512 (2009).

⁵Y. Nakai, K. Ishida, Y. Kamihara, M. Hirano, and H. Hosono, *J. Phys. Soc. Jpn.* **77**, 073701 (2008).

⁶H. Luetkens, H. H. Klauss, R. Khasanov, A. Amato, R. Klingeler, I. Hellmann, N. Leps, A. Kondrat, C. Hess, A. Köhler, G. Behr, J. Werner, and B. Büchner, *Phys. Rev. Lett.* **101**, 097009 (2008).

- ⁷F. Hunte, J. Jaroszynski, A. Gurevich, D. C. Larbalestier, R. Jin, A. S. Sefat, M. A. McGuire, B. C. Sales, D. K. Christen, and D. Mandrus, *Nature (London)* **453**, 903 (2008).
- ⁸T. Oka, Z. Li, S. Kawasaki, G. F. Chen, N. L. Wang, and G. Q. Zheng, *Phys. Rev. Lett.* **108**, 047001 (2012).
- ⁹Y. Ishida, T. Shimojima, K. Ishizaka, T. Kiss, M. Okawa, T. Togashi, S. Watanabe, X. Y. Wang, C. T. Chen, Y. Kamihara, M. Hirano, H. Hosono, and S. Shin, *Phys. Rev. B* **79**, 060503(R) (2009).
- ¹⁰A. V. Boris, N. N. Kovaleva, S. S. A. Seo, J. S. Kim, P. Popovich, Y. Matiks, R. K. Kremer, and B. Keimer, *Phys. Rev. Lett.* **102**, 027001 (2009).
- ¹¹A. Kondrat, G. Behr, B. Büchner, and C. Hess, *Phys. Rev. B* **83**, 092507 (2011).
- ¹²H.-F. Li, W. Tian, J.-Q. Yan, J. L. Zarestky, R. W. McCallum, T. A. Lograsso, and D. Vakhnin, *Phys. Rev. B* **82**, 064409 (2010).
- ¹³A. Schilling, M. Willemin, C. Rossel, H. Keller, R. A. Fisher, N. E. Phillips, U. Welp, W. K. Kwok, R. J. Olsson, and G. W. Crabtree, *Phys. Rev. B* **61**, 3592 (2000); B. Pümpin, H. Keller, W. Kündig, W. Odermatt, I. M. Savič, J. W. Schneider, H. Simmler, P. Zimmermann, E. Kaldis, S. Rusiecki, Y. Maeno, and C. Rossel, *ibid.* **42**, 8019 (1990).
- ¹⁴For a review, see P. A. Lee, N. Nagaosa, and X. G. Wen, *Rev. Mod. Phys.* **78**, 17 (2006), and references therein.
- ¹⁵T. T. M. Palstra, B. Batlogg, R. B. van Dover, L. F. Schneemeyer, and J. V. Waszczak, *Appl. Phys. Lett.* **54**, 763 (1989).
- ¹⁶R. H. Koch, V. Foglietti, W. J. Gallagher, G. Koren, A. Gupta, and M. P. A. Fisher, *Phys. Rev. Lett.* **63**, 1511 (1989).
- ¹⁷T. K. Worthington, F. H. Holtzberg, and C. A. Feild, *Cryogenics* **30**, 417 (1990).
- ¹⁸H. Q. Yuan, J. Singleton, F. F. Balakirev, S. A. Baily, G. F. Chen, J. L. Luo, and N. L. Wan, *Nature (London)* **457**, 565 (2009).
- ¹⁹J. Jaroszynski, F. Hunte, L. Balicas, Y.-J. Jo, I. Raicevic, A. Gurevich, D. C. Larbalestier, F. F. Balakirev, L. Fang, P. Cheng, Y. Jia, and H. H. Wen, *Phys. Rev. B* **78**, 174523 (2008).
- ²⁰E. D. Mun, M. M. Altarawneh, C. H. Mielke, V. S. Zapf, R. Hu, S. L. Budko, and P. C. Canfield, *Phys. Rev. B* **83**, 100514 (2011).
- ²¹E. D. Mun, N. Ni, J. M. Allred, R. J. Cava, O. Ayala, R. D. McDonald, N. Harrison, and V. S. Zapf, *Phys. Rev. B* **85**, 100502(R) (2012).
- ²²P. J. W. Moll, R. Puzniak, F. Balakirev, K. Rogacki, J. Karpinski, N. D. Zhigadlo, and B. Batlogg, *Nat. Mater.* **9**, 628 (2010).
- ²³J. Q. Yan, S. Nandi, J. L. Zarestky, W. Tian, A. Kreyssig, B. Jensen, A. Kracher, K. W. Dennis, R. J. McQueeney, A. I. Goldman, R. W. McCallum, and T. A. Lograsso, *Appl. Phys. Lett.* **95**, 222504 (2009).
- ²⁴T. Gebre, G. Li, J. B. Whalen, B. S. Conner, H. D. Zhou, G. Grissonnanche, M. K. Kostov, A. Gurevich, T. Siegrist, and L. Balicas, *Phys. Rev. B* **84**, 174517 (2011).
- ²⁵J. Bardeen and M. H. Stephen, *Phys. Rev.* **140**, A1197 (1965).
- ²⁶V. M. Vinokur, M. V. Feigel'man, V. B. Geshkenbein, and A. I. Larkin, *Phys. Rev. Lett.* **65**, 259 (1990).
- ²⁷P. Fulde and R. A. Ferrell, *Phys. Rev.* **135**, A550 (1964); A. I. Larkin and Yu. N. Ovchinnikov, *Sov. Phys. JETP* **20**, 762 (1965); Y. Matsuda and H. Shimahara, *J. Phys. Soc. Jpn.* **76**, 051005 (2007).
- ²⁸A. Gurevich, *Phys. Rev. B* **82**, 184504 (2010).
- ²⁹G. Blatter, M. V. Feigelman, V. B. Geshkenbein, A. I. Larkin, and V. M. Vinokur, *Rev. Mod. Phys.* **66**, 1125 (1994).
- ³⁰R. Prozorov, M. A. Tanatar, N. Ni, A. Kreyssig, S. Nandi, S. L. Budko, A. I. Goldman, and P. C. Canfield, *Phys. Rev. B* **80**, 174517 (2009).